Modeling JET ELMs with the SOLPS Edge Plasma Code

[1] F. Subba [2] P. Boerner [3] X. Bonnin [4] D. Coster [4] T. Eich [5] W. Fundamenski [4] A. Kallenbach [6] A. Loarte [5] G.F. Matthews [2] D. Reiter [1] F. Turco [1] R. Zanino, and JET EFDA Contributors

[1] *Dipartimento di Energetica, Politecnico, I-10129 Torino, Italy* [2] *Institute for Plasma Physics, Forschungszentrum Juelich GmbH, EURATOM Association, Trilateral Euregio Cluster, D-52425 Juelich, Germany* [3] *Max-Planck-Institut fuer Plasmaphysik, EURATOM Association, D-17491 Greifswald, Germany* [4] *Max-Planck-Institut fuer Plasmaphysik, EURATOM Association, D-85748 Garching, Germany* [5] *EURATOM-UKAEA Fusion Assoc., Culham Science Centre, Abingdon, Oxfordshire* [6] *EFDA-CSU, Max-Planck-Institut fuer Plasmaphysik, EURATOM Association, D-85748 Garching, Germany*

1 Introduction

SOL modelling is a key requirement to design the next generation of burning plasma experiments [1]. This is particularly true for Edge Localized Modes, because the energy released by an ELM in ITER could raise the target temperature above the tolerable limits. The simplest ELM models introduce ad-hoc transport multipliers. They should be carefully benchmarked against existing experimental data, before attempting any extrapolation to ITER. The ideal test case should be sufficiently well diagnosed to provide the input information required to define uniquely all the free parameters in the model, plus a set of additional measures to test the output. These are demanding conditions, often met only partially in practice. We illustrate the benchmark of the B2-solps5.0 code using an ELM from JET. In section 2 we describe the test case we chose, in section 3 we present our results and in section 4 we draw our conclusions.

2 Test case and model definition

We selected JET shot 55935, because of the high quality of experimental data available relative to the present standards. Inter ELM profiles reconstruction of n and T in the pedestal are available. At the targets, the D_α signal gives information on the particle flux with a time resolution of $\approx 10^{-4}s$, suitable to resolve the ELM transient. Triple Langmuir probes could give a cross check of the particle flux with comparable time resolution, but only a few are left at JET. The plasma configuration was optimized for the Infrared (IR) camera, which provided good quality divertor thermography. Coherent averaging [2] was applied to the IR data, obtaining a time resolution of $\approx 5 \times 10^{-5}s$.

For our modelling, we assume the plasma to be in steady state between successive ELMs. This is not strictly correct, but gives a convenient initial con-

dition to study the ELM transient, provided the rate of change of the plasma energy content is accounted for in the energy balance. NBI supplies $12MW$ of power, a fraction of which is unavailable for plasma heating due to prompt losses. Significant uncertainties also affect the bolometric measure of the core radiation. As a consequence, the power crossing the separatrix, P_{sep}, is not precisely known. Since P_{sep} influences significantly the target conditions [3], we can anyway use the latter for an *a posteriori* cross check. An input power $P_{in} \approx 6.5MW$ gives reasonable results. We inject $\Gamma_{in} \approx 3.5 \times 10^{21}s^{-1}$ from the core plasma to account for NBI and the core ionizations, and fix the separatrix density $n_{sep} \approx 2 \times 10^{19}m^{-3}$ by feedback controlling the gas-puff level, following the experimental practice. Not all the particle sinks are precisely accounted for, because the wall pumping efficiency is not known. We assume zero parallel velocity at the inner plasma boundary. Although this may not be strictly correct, numerical tests showed the assumption not to be critical. At the targets, we use the Bohm-Chodura conditions.

We model the plasma with the fluid approach but with a kinetic neutral model. Nowadays this is probably the best choice for 2D analysis in realistic geometry, even if it has some drawbacks. For example, hot electrons are expected to hit the targets during the early phase of an ELM [2, 4]. This is not presently included in our modelling.

3   Results

Figure 1 shows the radial diffusivities assumed to model the steady-state. In the absence of detailed knowledge, radial transport is a partially free parameter available to fit the experimental data. The depression at the separatrix agrees with the expected effect of the electric field [5]. Steady-state results are given by figures 2 (main plasma), 3 and 4 (targets). The least satisfactory is the inner target T_e . The low T_e at the strike point and a target to upstream total pressure ratio < 0.5 indicate at least partial detachment. A problem in the modelling could derive from an inaccuracy in the way the code splits the power between the two targets (e.g. due to not having included drift effects) or from some missing atomic and molecular physics. The lack of experimental points near the separatrix prevents from quantifying precisely the disagreement. Outer divertor thermography data, fig. 5, agree with numerical modelling in the SOL, but a plateau is found in the private region. This seems not consistent with the j_{sat} and T_e decay seen by the Langmuir probes, and needs further investigation.

We model the ELM by increasing D and χ for $6 \times 10^{-4}s$ to expel into the SOL $\approx 0.23MJ$ of energy and $\approx 23 \times 10^{19}$ particles. Fig. 6 compares measured and computed D_α signal from the divertor. Modelling is roughly con-

sistent with outer target data, but fails to reproduce the in/out asymmetry. At present, it is unclear whether the asymmetry is due to differences in the incoming particle fluxes or in the target response. Independent information on divertor particle fluxes can be given by the Langmuir probes, if the condition $3 \times T_e < V$ is satisfied. Fig. 7 shows the trace of j_{sat} recorded by probe 28 (outer) and three modelled traces, corresponding to different hypotheses on the strike point position. The green trace was computed assuming a shift of the separatrix position of 7 mm, the same assumption made for steady state modelling. The agreement is relatively good, but at the moment we consider it indicative only, because we do not have an accurate measurement of T_e at the target during the ELM and cannot determine the error bars affecting the measure. Unfortunately, we could not find a suitable equivalent probe at the inner target, which prevents from cross checking the particle flux asymmetry.

Two experimental estimates of the outer target power load, as a function of time and space, are compared with the computations in figs. 8 and 9. Modelling is consistent with the upper estimate of the power time evolution, while for the spatial profile we again note the existence of an unexpected plateau in the private region. The same remarks apply as for the steady state.

4   Conclusions

We applied B2-solps5.0 to study an ELM in JET, testing the potentialities for quantitative analysis. The lack of a complete theoretical understanding of the ELM phenomenon, the missing full assessment of experimental accuracy (error bars) and, sometimes, even the limited amount of experimental data, prevent for the time being a proper code validation. However, the numerical simulation does reproduce a few of the main features of an ELM, and has potentiality for further future improvements.

5   Acknowledgments

6   References

[1] ITER physics expert group, *Nucl. Fusion*, **39**, 2137, (1999).

[2] Pitts R., *ELM Driven Divertor Target Currents on TCV*, submitted to
    Nuclear Fusion.

[3] Pitcher C.S., et al., *Plasma Phys. Control. Fusion*, **39**, 779, (1997).

[4] Bergmann A., *Nucl. Fusion*, **42**, 1162, (2002).

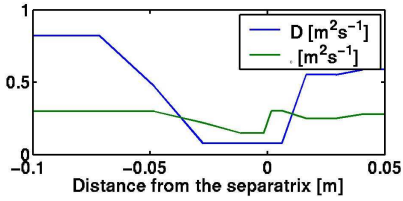[5] Rozhansky V., et al., *Nucl. Fusion*, **41**, 387, (2001).

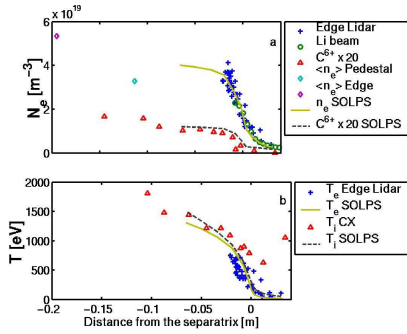Figure 1.   Particle (D) and energy (χ) diffusivity profiles

Figure 2.   a) Electron and C^{6+} density at the outer mid-plane. b) T_e and T_i profiles.
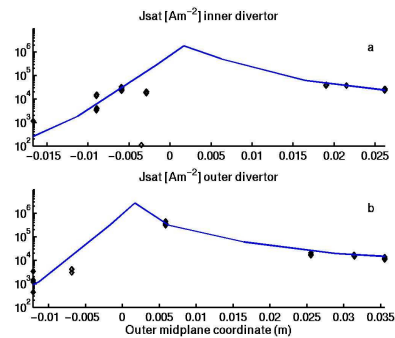
Figure 3. j_{sat} at a) inner target, b) outer target. The diamonds are Langmuir probes data collected in a period of 30 ms before the ELM
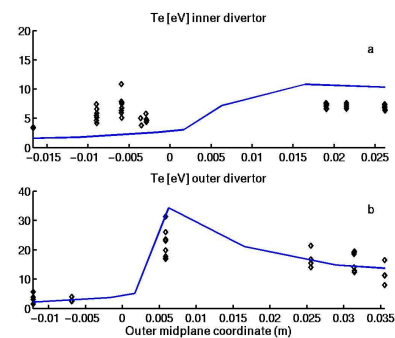
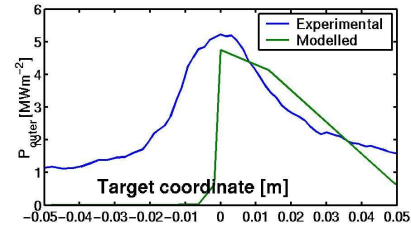Figure 4. T_e a) inner target, b) outer target. Diamonds are as in figure 3

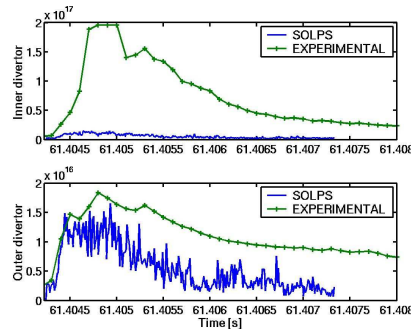Figure 5.   Outer divertor heat flux profile in stationary conditions from model and Infra Red themography

Figure 6. D_α signal at the inner and outer divertor. The code fails to reproduce the target asymmetry
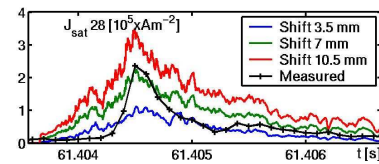
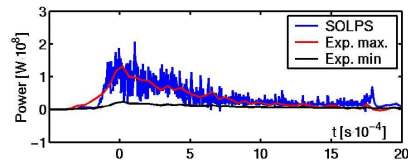Figure 7. j_{sat} measured and computed during the ELM for an outer divertor probe.

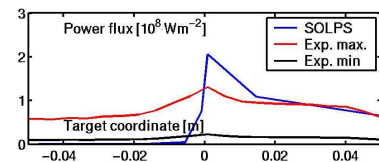Figure 8.   Evolution of the power onto the outer divertor during the ELM.

Figure 9.   Heat flux deposition profile onto the outer divertor at the time of the peak.